ELSEVIER

In Collaboration with the
Royal Netherlands Institute
for Sea Research

Journal of Sea Research 55 (2006) 3–14

JOURNAL OF SEA RESEARCH

www.elsevier.com/locate/seares

Effects of mussel filtering activity on boundary layer structure

Luca A. van Duren *, Peter M.J. Herman, Adri J.J. Sandee, Carlo H.R. Heip

Netherlands Institute of Ecology, Centre for Estuarine and Marine Ecology, PO Box 140, 4400 AC Yerseke, the Netherlands

Received 15 July 2005; accepted 2 August 2005

Abstract

The structure of the benthic boundary layer over a bed of mussels (*Mytilus edulis*) was investigated in a large racetrack flume. Flow was observed to be modified both by the physical roughness of the mussel bed and by the momentum input of the exhalent jets of the mussels. Particularly when the mussels were closed, and filtering activity was reduced to a minimum, we observed an internal boundary layer, around 4 cm thick, within the log layer. This internal boundary layer was often masked when the mussels were filtering actively. The presence of an internal boundary layer indicates that the boundary layer is not only structured by friction drag, but that form drag due to roughness elements also plays an important role. Consequently, estimates of bed shear stress based on velocity or Reynolds stress measurements carried out more than a few cm above the bed may be inaccurate.

Over inactive mussels the shear velocity in the internal boundary layer (the roughness sub-layer) is smaller and bed shear stress is consequently reduced. Filtration activity of the mussels increased the velocity gradient in the lower layer at low and intermediate velocities, but at higher flow rates velocity profiles were not affected. Clear effects of the exhalent jets on absolute levels of TKE could be measured at all ambient velocities, while the effect on the Reynolds stress was limited. Velocity normalised TKE and Reynolds stress also indicated that the effect of the siphonal currents was limited at high velocities.

Our results indicate that mussel filtration activity may have an important effect on exchange processes at the sediment-water interface, but that the extent of the effect is highly dependent on the ambient flow conditions.

Keywords: Benthic boundary layer; Roughness; Feeding currents; *Mytilus edulis*; Turbulence; Flow

1. Introduction

It is now widely appreciated that small-scale interactions between benthic organisms and their environment have large-scale effects on the geomorphology of the seabed (Murray et al., 2002). Processes such as erosion and sedimentation are determined by local hydrodynamics. Velocity gradients close to the bottom, and levels of turbulence are influenced by the bottom morphology. Certainly in relatively shallow ecosystems bottom roughness is for a large part determined by biogenic structures (Wright et al., 1997a,b). These may either be structures that are built or constructed by animals (such as mounds or tubes of bottom-dwelling worms) or they may consist of the

---

* Corresponding author.
E-mail address: l.vanduren@nioo.knaw.nl (L.A. van Duren).

1385-1101/$ - see front matter © 2005 Elsevier B.V. All rights reserved.
doi:10.1016/j.seares.2005.08.001

organisms themselves (such as seagrass meadows or shellfish beds). Roughness elements tend to slow down the current velocities close to the bed and generate turbulence. Benthic filter feeders such as the blue mussel (*Mytilus edulis*) form large dense aggregates with a hard, rough structure. Such structures will in general introduce turbulence into the bottom boundary layer (Butman et al., 1994).

Flow velocity in the benthic boundary layer (bbl) is generally assumed to show a logarithmic velocity profile, which is referred to as the 'law of the wall':

$$\bar{u}_{(Z)} = \frac{u_*}{\kappa} \ln \frac{z}{z_0} \tag{1}$$

where $\bar{u}_{(z)}$ is the mean velocity at height z, u_* is the shear velocity, κ is the Von Karman constant ($k \approx 0.41$), z is the distance from the bottom and z_0 is the roughness length. The roughness length is often assumed to relate to the size of the roughness elements on the bottom by a factor 1/30 (Dade et al., 2001). The law of the wall is based on the assumption that the benthic boundary layer is shaped by viscous drag. This approximation holds in situations where the roughness elements are relatively small. When roughness elements increase in size, form drag may start to play a role (Arya, 1975; Chriss and Caldwell, 1982). Turbulent wake structures can form behind the roughness elements, which can result in internal boundary layers, each with a different shear velocity.

However, mussels and other bivalves are not merely dead roughness structures. Mussels gather food by drawing water in, pumping it over their gills and expelling it again through their exhalent siphons (Wildish and Kristmanson, 1997). Each individual mussel can process several litres of water per hour (Hildreth, 1976; Riisgård, 1991). Prins et al. (1996) determined that in the Oosterschelde estuary (the Netherlands) mussel beds process 1.3–7.1 m^3 water m^{-2} h^{-1}. The exhalent jets contain some momentum (O'Riordan et al., 1995). Besides preventing once filtered water from re-entering the filter feeding animal, the complementary function of the exhalent jets may be to mix the near-bottom water (Larsen and Riisgard, 1997). The question is whether this momentum input in the water column is sufficient to influence the boundary layer structure, and consequently transport processes in the boundary layer.

This study aims to investigate the general structure of the benthic boundary layer over a dense bed of actively filtering mussels *M. edulis* and to assess the effect and extent of the filtration action of the mussels on the flow morphology at different flow velocities.

2. Material and methods

2.1. The flume tank

Experiments were carried out in a large racetrack flume at the NIOO laboratory in Yerseke. The flume consists of a large oval channel with a total length of 17.55 m, a straight working section of 10.8 m and a total capacity of about 10 m^3. The channel measures 60 cm in width and water depth is maintained at 40 cm.

Water flow is generated by a conveyor belt system, acting as a paddle wheel. The conveyor belt is driven by an engine which can be set to operate at a frequency between 0 and 60 Hz. The bends at either end of the flume have an outer diameter of 3.25 m. In these bends the water flow is guided through 4 subchannels by turning vanes. Downstream of the conveyor belt and immediately at the start of the test section, the water passes through a stack of PVC tubes (Ø 2 cm) acting as collimators.

A carriage with a 3D positioning system can be placed anywhere along the length of the working section. The 3D positioning system can move over the total width and depth of the flume and over a maximum length of 70 cm in the direction of the main flow. The latter axis is defined as the x-axis, the y-axis is defined horizontally, across the main flow and the z-axis is defined as the vertical axis.

2.2. Morphology and maintenance of the mussel bed

On 17 March 1998, a mussel bed was created by transferring box cores from a mussel bed in the Oosterschelde to the working section of the flume. The experimental mussel bed had a distinct leading edge, behind which the mussels covered the complete ground area of the flume over a total length of 3.3 m. The base of the mussels was level with the flat bottom of the working section. We used the distance-to-boundary function of the ADV to determine the height of the mussel bed in several locations. Average mussel bed height was 61 mm, the actual height ranging from 49 to 86 mm. Average density during the experiments was around 1800 mussels m^{-2}, average shell length was 38.5 mm (standard deviation: 8.3 mm). When these experiments were carried out, the experimental mussel bed had already been in the flume for several months and had a stable configuration. Changes in average height of the bed in response to changes in food or flow conditions, as reported by Butman et al. (1994), were not observed, or at least not detectable with the ADV.

During this experimental period, the mussels were fed on finely ground commercially available flake fish food (Tetramin®) which is a mixture of animal–derived material and vegetable matter (including algae) and added vitamins.

2.3. Flow measurements

Flow measurements were carried out with an Acoustic Doppler Velocimeter (ADV; Nortek field version), mounted on the 3D positioning system and set to operate at a rate of 25 Hz. In the coordinate system of the carriage, x was defined as the direction along the main flow direction, y across the flume channel and z the vertical direction. Before each experiment the flume was seeded with very fine deep–sea clay sediment, which stays in suspension, even at very low flow velocities. To compensate for loss of seeding material due to filtration by the mussels, a continuous trickle of sediment suspension was added to the flume during experiments, keeping seeding levels more or less constant, and at all times above the threshold level necessary for the ADV measurements. Other tests have indicated that this sediment may affect mussel filtration rates, but only at much higher concentrations than were used in the current experiments.

Three flow rates were chosen: low, intermediate and high, corresponding to free–stream velocities over the flat flume bottom, in front of the mussel bed of around 45, 100 and 275 mm s^{-1}, respectively, and over the mussel bed of 55, 130 and 350 mm s^{-1}, respectively. The difference results from the fact that due to the presence of the mussels the cross-sectional area of the flume over the mussels was slightly smaller than over the test section upstream of the mussel bed.

Experiments consisted of detailed vertical profiles, at one specified x-y co-ordinate. We defined z=0 to be the average height of the mussel bed. Each profile contained 24 points the highest one at 180 mm above the bed. The ADV collected 8250 measurements at each point, at a rate of 25 Hz.

From the total amount of measurements at one given point the averages of the individual velocity components u, v and w (corresponding to the velocities in x, y and z direction) were calculated as well as the vertical flux of momentum, the Reynolds stress $(\rho\overline{u'w'})$ and turbulent kinetic energy (TKE, $0.5^*(\overline{u'}^2+\overline{v'}^2+\overline{w'}^2)$).

2.4. Experimental protocol

Prior to each experiment the mussels were starved for 2 to 3 d, until all were nearly shut and filtration activity was minimal (Fig. 1A). During the starvation period the flume was set to run at experimental velocity to prevent the mussels from reacting to a change in flow velocity.

At 1.5 m downstream of the leading edge, in the middle of the flume channel, an area of 10 × 10 cm

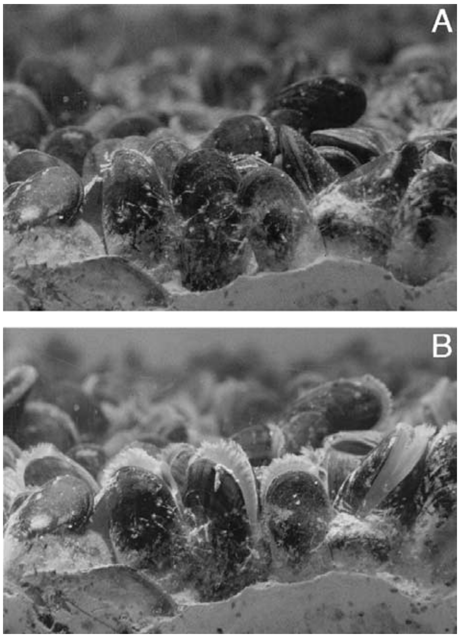

Fig. 1. Mussels in the flume: (A) mussels virtually closed and inactive, (B) mussels 15 min after food supply, open and actively filtering.

was selected. Earlier experiments had shown that at this location the thickness of the boundary layer, as well as the turbulence profiles did not change appreciably in the along-stream direction. Using the 'distance to boundary' function of the ADV, in this area the height of the mussel bed was determined every cm in the x and y direction. A location within this area was selected where the height of the mussel bed coincided with the average height of the mussels. Here the ADV was set to measure a vertical profile with the mussels in this nearly inactive state. After completion of this profile, food (Tetramin) was distributed evenly over the flume. After 15 min, when all the mussels were wide open and filtering actively (Fig. 1B), a second vertical profile was measured at the same location in the flume.

In addition to the profiles over the mussels, one profile was collected at each of the three experimental velocities, upstream of the mussel bed, at the centre of the flume, over the flat fibreglass bottom surface.

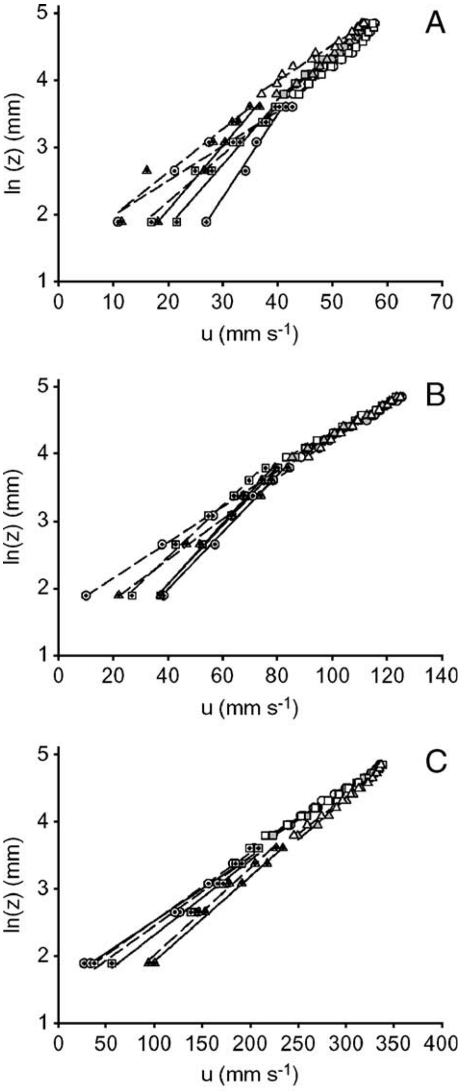

Fig. 2. Boundary layer structure over active and inactive mussels at three velocities: (A) low velocity, (B) intermediate velocity, (C) high velocity. Grey symbols and solid regression lines: closed, inactive mussels; open symbols with dashed regression lines: open, active mussels. The symbols with a crosshair indicate the points in the lower boundary layer. The different symbol shapes indicate the replicate experiments.

3. Results

At the low flow velocity a marked difference was observed in the velocity profiles measured over nearly inactive and actively filtering mussels, particularly in the lower water layers (Fig. 2A). A velocity profile of an ideal boundary layer shows a single straight line, when the horizontal velocities are plotted against a logarithmic z-axis. The flow over the mussels often did not show one single log-layer, but for each profile two regression lines have been calculated on the basis of a clear break in the lines. Such a change in the velocity gradient is called an internal boundary layer and is common over rough surfaces (Chriss and Caldwell, 1982). A homogeneity-of-slopes test shows a clear internal boundary layer ($p<0.001$) over inactive mussels, but in the actively filtering mussels there is no statistical difference between the slopes of the upper and lower layer. The higher part of the boundary layer was not affected by the behaviour of the mussels, but in the lower 4.5 cm the horizontal flow velocity was lower over the actively filtering mussels than over the inactive ones. This resulted in a steeper velocity gradient over the active animals compared to the inactive mussel bed. The intermediate velocity showed the same pattern (Fig. 2B). A very clear breakpoint in the regression lines can be observed in the experiments over closed mussels, but in the actively filtering mussels this breakpoint is much less clear, although still significantly different. At the high velocity we could still observe an internal boundary layer, although it was not as pronounced as at lower velocities (Fig. 2C). However, neither in the lower, nor in the upper layer was there any significant difference between actively filtering and inactive mussels. The high ambient velocity masked the effect of the exhalent jets. Table 1 shows an overview of the estimates of u_* (derived from the slope of the semi log plot of u against z) and z_0 (derived from the intercept of the extrapolated regression line with the z-axis).

In comparison with the flat flume bottom, inactive mussels increase turbulence levels and therefore local mixing. The slight differences in free-stream velocity over flat bottom and the mussel bed are far too small to account for the observed differences. The pooled profiles of TKE show a clear effect of the exhalent jets on turbulence levels throughout the water column. The effect is pronounced at all velocities, even at the highest free stream velocity (Fig. 3A, B and C). The presence of mussels also increases the flux of momentum towards the bed (Fig. 4A, B and C). However, despite the pronounced effect on TKE, the filtration activity of the mussels has relatively little effect on the Reynolds stress at any of the experimental velocities (Fig. 4A, B and C). To evaluate the relative effect of the presence of mussels in general and the exhalent jets in particular on turbulence at different flow velocities, we normalised both TKE and

Table 1
Values for shear velocity, roughness length and bottom shear stress

		u_* (mm s^{-1})		z_0 (mm)		τ_o (Pa)
Low velocity						
flat bottom		2.20		0.02		0.005
mussels	layer	average	standard error	average	standard error	
open	lower	6.70	0.63	3.42	0.64	0.05
	upper	6.45	0.65	3.49	1.50	0.04
shut	lower	4.00	0.35	0.77	0.28	0.02
	upper	6.13	0.13	2.81	0.19	0.04
Intermediate velocity						
flat bottom		5.93		0.12		0.04
mussels	Layer	average	standard error	average	standard error	
open	Lower	13.21	1.39	3.62	0.74	0.18
	Upper	17.37	0.95	6.75	1.05	0.31
Shut	Lower	9.35	0.18	1.31	0.03	0.09
	Upper	17.54	0.06	6.87	0.12	0.31
High velocity						
flat bottom		15.25		0.06		0.24
Mussels	Layer	average	standard error	average	standard error	
Open	Lower	37.42	2.90	3.55	0.77	1.43
	Upper	43.96	3.47	5.34	1.26	1.98
Shut	Lower	37.46	3.05	3.33	0.82	1.43
	Upper	41.07	3.71	4.41	1.23	1.72

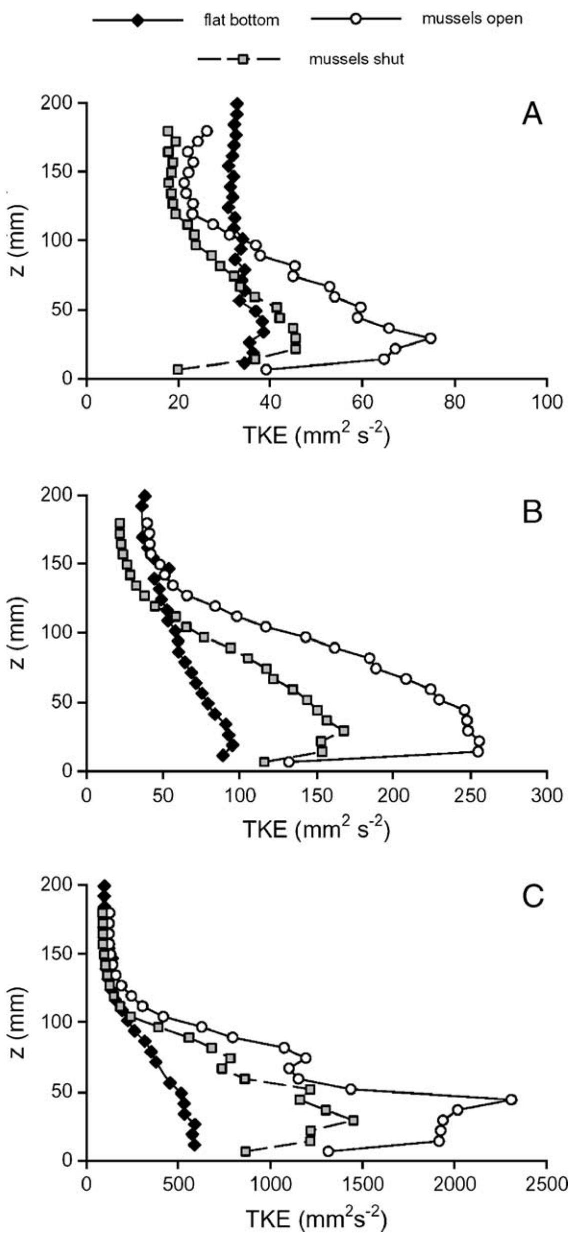

Fig. 3. TKE over active and inactive mussels: (A) low velocity, (B) intermediate velocity, (C) high velocity. The graphs represent the average of the three replicate experiments.

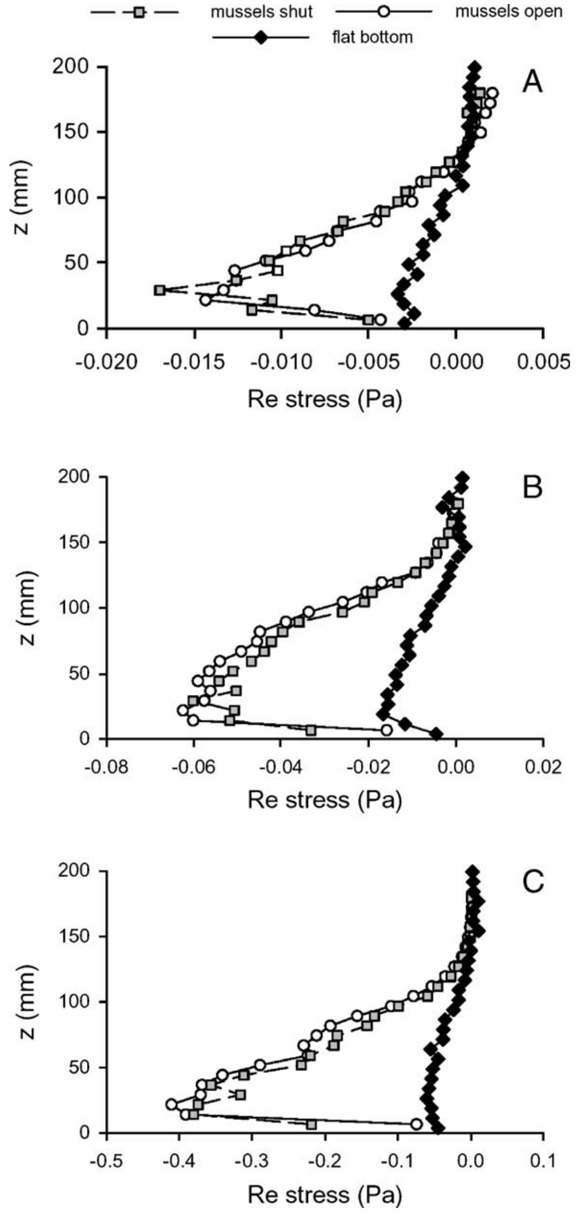

Fig. 4. Reynolds stress $\rho\overline{u'w'}$ over active and inactive mussels: (A) low velocity, (B) intermediate velocity, (C) high velocity. The graphs represent the average of the three replicate experiments.

Reynolds stress using the square of the local velocity magnitude (Fig. 5A and B, respectively). As turbulence production in the boundary layer should scale with the square of the local velocity magnitude, this normalisation will allow a direct comparison of effects between velocities. Close to the bed the turbulence intensity is an order of magnitude larger over mussels in comparison to the flat bottom. Over closed, inactive mussels the profiles of normalised TKE at different velocities match each other closely. Over actively filtering mussels TKE is clearly higher than over closed ones and the effect is less at the highest velocity. The velocity normalised Reynolds stress shows an enhancing effect of the mussel activity in the lowest layers at the low and intermediate velocity, but little effect at the high velocity. As with the TKE, the values of normalised Reynolds stress over the flat bottom are small in comparison with those over mussels, either open or closed.

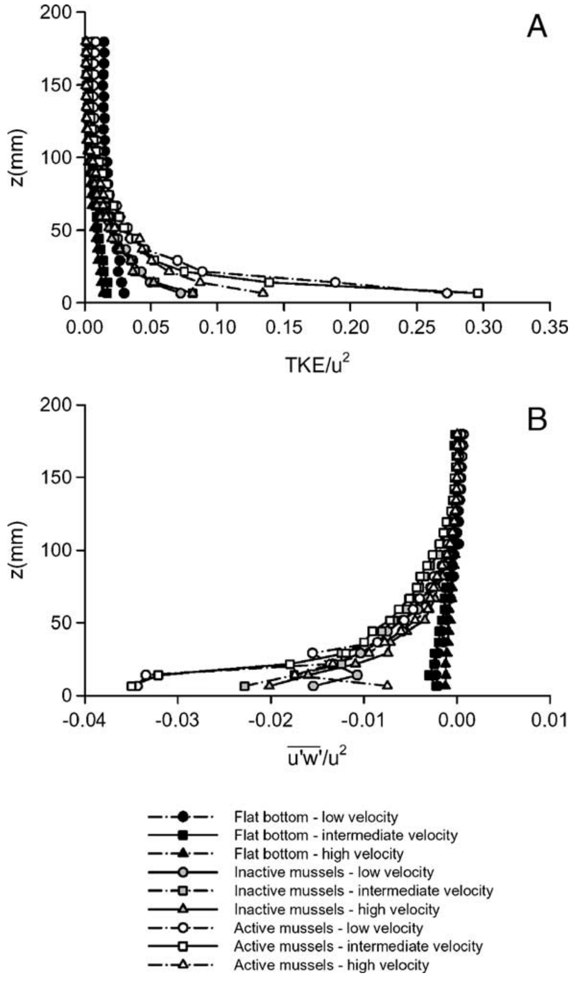

Fig. 5. (A) Velocity normalised TKE, and (B) Reynolds stress over active and inactive mussels.

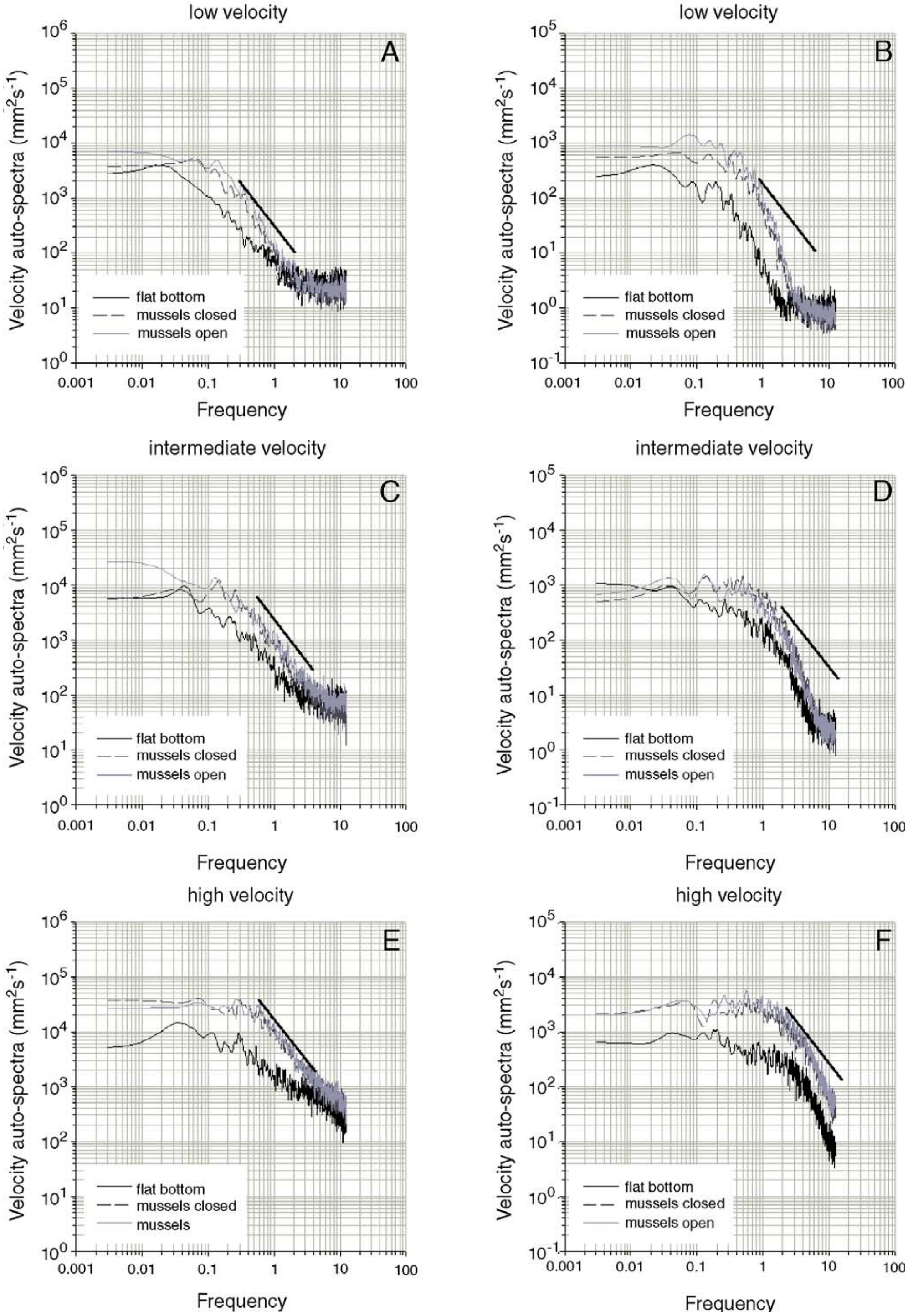

Fig. 6. Velocity autocorrelation graphs of the u (A, C and E) and w (B, D and F) velocity component. (A and B) low velocity, (C and D) intermediate velocity, (E and F) high velocity.

Fig. 6A to F shows the velocity autocorrelation graphs of the u and w component at a height of 1.5 cm over the bed. This height was selected because it was as close as possible to the mussel bed, without any possibility of the ADV measuring volume overlapping with protruding mussels. For each velocity one graph is shown for the flat bottom, one for closed, inactive mussels and one graph for open actively filtering mussels. The three replicates at each velocity match each other closely. At all velocities a clear inertial subrange is recognisable. In the u velocity component the decline in the inertial subrange is close to $-5/3$, conforming to the Kolmogorov law. The decline in the w component is somewhat steeper, particularly at the low velocity. There is little difference between the open and the closed mussels; however, there is a clear difference between mussels and the flat bottom. The mussels are unlikely to introduce very large eddies into the water column, but we also could not observe any distinct peaks in the middle to lower part of the inertial subrange, attributable to wake effects of the exhalent currents. At the high velocity the 25 Hz measuring frequency of the ADV was just not sufficient to resolve the Kolmogorov length scale.

4. Discussion

4.1. Internal boundary layer

The theory of a single logarithmic velocity profile in the benthic boundary layer assumes that the velocity gradient is the result of friction drag alone. This assumption is only valid when the roughness elements on the bottom (sediment grains, ripples or biogenic structures) are small enough so they remain submerged in the viscous sub-layer. When roughness elements are large enough to generate turbulent wake structures, the 'standard' description of a single log layer may no longer hold (Chriss and Caldwell, 1982). The mussel bed in our flume had an average height of 61 mm above the flume bottom, but because the mussels were very closely packed together we cannot consider this to be the size of the roughness elements. The difference between the highest and the lowest point on the mussel bed was 37 mm, so 25–30 mm is probably a more reasonable estimate of the average roughness height. This is still clearly enough to cause an internal boundary layer. Similar profiles have been reported by Nikora et al. (1997) over a rough bottom surface in a flume tank. They named the lower logarithmic layer the near-bed 'roughness sub-layer' showing a smaller velocity gradient than the upper logarithmic layer. Nikora et al. (2002) also reported internal boundary layers in the field over beds of horse mussels, *Atrina zelandica,* in the field.

Modellers often assume a single log layer in boundary layer flow (Butman et al., 1994). According to Nikuradse's parameterisation of bed roughness, the roughness length (z_0) is equal to one thirtieth of the actual size of the roughness elements (Schlichting, 1979; Butman et al., 1994). On the basis of the height differences over our mussel bed we would expect to see a z_0 of around 1 mm, but particularly our estimates of z_0 on the basis of the regression lines in the upper layer were substantially higher. Assuming a value for z_0, purely on the basis of the size of the roughness elements can lead to underestimation of mixing in the higher layers. Field studies often rely on a limited amount of velocity and turbulence measurements, not very close to the bed. This has other consequences for the interpretation of flow data for obtaining information on bed shear stress and particle transport or particle entrainment calculations. Particularly over the inactive mussels, u_* was 1.5 to almost 2 times higher in the upper layer than in the lower. Since τ_0 relates to u_*^2, this could lead to a significant overestimation of bed shear stress values (Chriss and Caldwell, 1982).

The profiles of TKE and Reynolds stress show that within the boundary layer these parameters are not constant, as is often assumed (Kim et al., 2000). The assumption of constant stress in the boundary layer is often used to estimate bottom shear stress in the field. According to Tennekes and Lumley (1999) $u_*^2 = -\overline{u'w'}$. In a simple single log layer there is also a simple linear relationship between TKE and bed shear stress (Kim et al., 2000). Soulsby and Dyer (1981) already indicated that these approximations are poor in accelerating flow. These relationships apparently also break down over rough biogenic structures such as mussel beds.

4.2. Effect of behaviour

The activity of the mussels affected only the velocities in the lower logarithmic layer (or the roughness sublayer). The effect was more pronounced at lower flow velocities. Over inactive mussels, the near-bed logarithmic layer always showed smaller velocity gradients. As velocity gradients, rather than velocity per se, are responsible for transmission of forces from the water to the bed, this implies less shear stress. Mussel activity removed momentum from the near-bed layer, increasing the velocity gradient in the lower layer. At low and intermediate flow velocities, the gradients close to the bed were similar to those in the upper layer.

Mussel activity appeared to have little effect on the shear velocity in the upper logarithmic layer. However, since particularly the near-bed region may be affected, this may influence particle dynamics and resuspension processes. Critical bottom shear stress for resuspension of sediment in a flume was established to be around 0.10–0.14 Pa (Wright et al., 1997b). In their turbidity models, Burchard and Baumert (1998) use 0.13 Pa as the resuspension threshold for suspended particulate matter, and 0.10 Pa as the threshold for sedimentation. At the lowest velocity we used ($u_\infty = 55$ mm s^{-1}), τ_0 is always below these thresholds and at the highest velocity ($u_\infty = 350$ mm s^{-1}), τ_0 always exceeds the critical erosion threshold, regardless of whether the mussels are active or inactive. However, at the intermediate flow ($u_\infty = 130$ mm s^{-1}), τ_0 is 0.09 Pa when the mussels are inactive but 0.18 Pa when they are actively feeding. At a limited range of ambient flow velocities shellfish filtration activity may determine whether particulate matter settles or remains in suspension.

Although the steepness of the velocity gradient was affected only at low and intermediate velocity in the lower part of the boundary layer, effects on TKE were measurable even at the highest velocity up to 10 cm high into the water column. However, the effects on the vertical flux of momentum $\left(\rho\overline{u'w'}\right)$ were not at all spectacular. Ertman and Jumars (1988) found that the wakes of the siphonal currents of *Clinocardium nuttallii* increased variability in deposition of particles downstream of the bed, but that the jets did not influence the mean deposition rate over the bed. However, O'Riordan et al. (1993) concluded that the exhalent jets of the mussels decreased refiltration rates by increasing the vertical flux of phytoplankton.

The fact that mussels and other biogenic structures have a significant effect on local hydrodynamics, and consequently on sedimentation and erosion processes, is well documented (Abelson et al., 1993; Jumars and Nowell, 1984; Wright et al., 1997a). Whether or not biologically generated currents have consequences for the flux of particulate material to the bed will depend on the strength of the exhalent jets in relation to the ambient flow field. If we consider an individual mussel to be a pump, the useful power, delivered by this pump ranges around 10μW for a 'standard mussel' (Riisgård and Larsen, 2001). This standard mussel measured 35 mm in shell length, close to our mussels. According to Jørgensen et al. (1986), about 28% of the power is taken up by the kinetic energy in the exhalent jets, which is the power that is transferred to the overlying water column. Our mussel bed contained about 1800 mussels m^{-2}, consequently this mussel bed should transfer about 5 mW m^{-2} to the boundary layer, when the mussels are all actively filtering. Another way of roughly estimating the kinetic energy flux is based on the jet speed. Our mussels had an average dry weight of 0.16 g. Using the relationship described by Møhlenberg and Riisgård (1979) we assume that each of the 1800 mussels m^{-2} filters on average 3 litre per hour and has an exhalent siphon diameter of 4 mm. This yields a jet speed of 0.066 m s^{-1}, resulting in a kinetic energy flux of 3.3 mW m^{-2}, i.e. a value of the same order of magnitude. If we assume that the kinetic energy in the jet is almost instantly converted into turbulent kinetic energy, and that this energy predominantly dissipates in the lower 5 cm of the boundary layer, we can estimate the average TKE production rate by the mussels to be 0.07 W m^{-3}. These figures have to be treated with great caution, though, since all these calculations depend on numerous assumptions. However, it is encouraging that the estimate of energy flux by the mussels through the power delivery of the mussel pump and the estimate via the exhalent siphons yield such similar figures.

The rate of production of TKE in the bottom boundary layer can be estimated as:

$$P = -\overline{u'w'} * (\partial\bar{u}/\partial z) \tag{2}$$

(Tennekes and Lumley, 1999). For our low, intermediate and high flow velocities we get values of: 0.008, 0.08 and 1.1 W m^{-3}, respectively. This would lead us to conclude that at the low velocity, the TKE production due to the mussel filtration activity is greater than the generation due to bottom shear. At the intermediate velocity, the values are of a similar order of magnitude, while at high velocities the contribution of the mussel activity is negligible. This appear to tie in neatly with our observation that at low and intermediate velocities the shape of the boundary is appreciably affected, while at high velocity there appears to be no difference between active or inactive mussels. However, in the TKE profiles we measure clear effects in the near-bed TKE levels, even at the highest velocities. Fig. 3 indicates that the effect of the exhalent jets on TKE is not a simple additive process, since in absolute terms, the increase in TKE in the near-bed layer is largest at the highest velocity. Of course we cannot completely exclude the possibility that the bed with open mussels has a slightly rougher topography than the bed with closed mussels, and that this extra roughness contributes to the increased near-bed turbulence. However, this effect can only be slight and subtle. The difference is not measurable with e.g. the surface-detection mode of the ADV. The TKE increase in e.g. the intermediate velocity (Fig. 3B) between open and closed mussels is of the same order of magnitude as the difference between a flat smooth surface and inactive mussels. We therefore have to conclude that the bulk of this effect is not due to topographical differences between open and closed mussels.

The fact that the Reynolds stress $\left(\rho \overline{u'w'}\right)$ is not significantly affected by the jets indicates that the turbulent eddies created by the jets are uncorrelated and lose their energy on a time-scale shorter than the time taken by larger eddies to strain smaller ones (Belcher et al., 1993). The jets appear to be acting as an additional source of form drag (Lu et al., 2000). This is again an indication that the standard law-of-the-wall approach, which assumes that the boundary layer is shaped by friction drag, is too simplistic for small-scale processes over biogenic structures. In these situations the normal relationships between parameters such as u_*, $\left(\rho \overline{u'w'}\right)$ and $0.5*\left(\overline{u'^2}+\overline{v'^2}+\overline{w'^2}\right)$ that are often used to estimate one parameter from the other (Kim et al., 2000) tend to break down (Lu et al., 2000).

Ertman and Jumars (1988) observed that siphonal currents of the cockle *Clinocardium nuttallii* acted as vertical cylindrical objects in the boundary layers, shedding wakes. So, these exhalent jets basically act as additional roughness elements. In the autocorrelation spectrum, we were unable to detect any peaks that we could attribute to wakes of exhalent jets. We should point out that we only measured 3 profiles over filtering mussels at each velocity. The wakes will also dissipate very quickly so close to the bed. At low velocities, when the exhalent jets are most likely to penetrate higher up into the water column, the wake vortices will probably only be measurable immediately downstream of an exhalent jet. It is therefore quite conceivable that we missed such a crucial spot. Another possible explanation for the absence of a wake signal in the spectral analysis is that due to the density of the mussel bed, the exhalent currents interact, and therefore will simply not produce a clearly identifiable peak. It is probably still a valid concept to consider the action of exhalent jets on boundary layer flow as additional roughness. It is clear that the estimates of z_0 in the lower part of the boundary are much affected by the mussel activity, particularly at lower velocities.

It has already been shown that the filtration activity of mussels influences food availability of mussels downstream in a mussel bed (Butman et al., 1994). Mussel filtration activity is also clearly influenced by food availability (Riisgård, 1991; Newell et al., 2001; Widdows et al., 2002). We used the latter to compare flow profiles over active and inactive mussels. Food availability is not only influenced by food concentration in the water, but also by the local hydrodynamics. Mussel pumping rates are not only affected by food concentration, but also by silt concentration (Kiørboe et al., 1981) and by hydrostatic pressure (Hildreth, 1976; Beukema and Essink, 1986; Famme et al., 1986). The latter process is still under some dispute. Some authors found that pressure effects at high flow rates can reduce filter capacities of bivalves (Wildish and Miyares, 1990); however, others found no decline in filtration rates with increasing flow (Widdows et al., 2002) The interaction between these parameters and near-bed flow processes deserves further attention. Also the issue of possible effects of modification of topography, combined with the effects of exhalent jets is not yet completely resolved (Widdows and Brinsley, 2002). Perhaps more fine-scaled bottom scanning techniques to quantify bed roughness (Springer et al., 1999) combined with other flow visualisation techniques such as PIV (Stamhuis and Videler, 1995) can help elucidate this intricate bio-fluid-dynamics issue.

Acknowledgements

We would like to thank John Simpson and Filip Meysman for the fruitful discussions on this topic. This is publication 3606, NIOO-KNAW Netherlands Institute of Ecology. This work was funded by the EU ELOISE project PhaSE (contract nr.: MAS3-CT96-0053).

References

Abelson, A., Miloh, T., Loya, Y., 1993. Flow patterns induced by substrata and body morphologies of benthic organisms and their roles in determining availability of food particles. Limnol. Oceanogr. 38, 1116–1124.

Arya, S.P.S., 1975. A drag partition theory for determining the large-scale roughness parameter and wind stress on the Arctic pack ice. J. Geophys. Res. 80, 3447–3454.

Belcher, S.E., Newley, T.M.J., Hunt, J.C.R., 1993. The drag on an undulating surface induced by the flow of a turbulent boundary-layer. J. Fluid Mech. 249, 557–596.

Beukema, J.J., Essink, K., 1986. Common patterns in the fluctuations of macrozoobenthic species living at different places on tidal flats in the Wadden Sea. Hydrobiologia 14, 199–207.

Burchard, H., Baumert, H., 1998. The formation of estuarine turbidity maxima due to density effects in the salt wedge. A hydrodynamic process study. J. Phys. Oceanogr. 28, 309–321.

Butman, C.A., Fréchette, M., Geyer, W.R., Starczak, V.R., 1994. Flume experiments on food supply to the blue mussel *Mytilus edulis* L. as a function of boundary layer flow. Limnol. Oceanogr. 39, 1755–1768.

Chriss, T.M., Caldwell, D.R., 1982. Evidence for the influence of form drag on bottom boundary layer flow. J. Geophys. Res. 87, 4148–4154.

Dade, W.B., Hogg, A.J., Boudreau, B.P., 2001. Physics of flow above the sediment-water interface. In: Boudreau, B.P., Jørgensen, B.B. (Eds.), The Benthic Boundary Layer, vol. 2. Oxford University Press, Oxford, pp. 4–37.

Ertman, S.C., Jumars, P.A., 1988. Effects of bivalve siphonal currents on the settlement of inert particles and larvae. J. Mar. Res. 46, 797–813.

Famme, P., Riisgård, H.U., Jørgensen, C.B., 1986. On direct measurement of pumping rates in the mussel *Mytilus edulis*. Mar. Biol. 92, 323–327.

Hildreth, D.I., 1976. The influence of water flow rate on pumping rate in *Mytilus edulis* using a refined direct measuring apparatus. J. Mar. Biol. Ass. UK 56, 311–319.

Jørgensen, C.B., Famme, P., Saustrup Kristensen, H., Larsen, P.S., Møhlenberg, F., Riisgård, H.U., 1986. The bivalve pump. Mar. Ecol. Prog. Ser. 3, 69–77.

Jumars, P.A., Nowell, A.R.M., 1984. Effects of benthos on sediment transport: difficulties with functional grouping. Cont. Shelf Res. 3, 115–130.

Kim, S.C., Friedrichs, C.T., Maa, J.P.Y., Wright, L.D., 2000. Estimating bottom stress in tidal boundary layer from Acoustic Doppler Velocimeter data. J. Hydrol. Eng. 126, 399–406.

Kiørboe, T., Møhlenberg, F., Nøhr, O., 1981. Effect of suspended bottom material on growth and energetics in *Mytilus edulis*. Mar. Biol. 61, 283–288.

Larsen, P.S., Riisgard, H.U., 1997. Biomixing generated by benthic filter feeders: a diffusion model for near-bottom phytoplankton depletion. J. Sea Res. 37, 81–90.

Lu, Y.Y., Lueck, R.G., Huang, D.Y., 2000. Turbulence characteristics in a tidal channel. J. Phys. Oceanogr. 30, 855–867.

Møhlenberg, F., Riisgård, H.U., 1979. Filtration rate, using a new indirect technique in thirteen species of suspension feeding bivalves. Mar. Biol. 54, 143–147.

Murray, J.M.H., Meadows, A., Meadows, P.S., 2002. Biogeomorphological implications of microscale interactions between sediment geotechnics and marine benthos: a review. Geomorphology 47, 15–30.

Newell, C.R., Wildish, D.J., MacDonald, B.A., 2001. The effects of velocity and seston concentration on the exhalant siphon area, valve gape and filtration rate of the mussel *Mytilus edulis*. J. Exp. Mar. Biol. Ecol. 262, 91–111.

Nikora, V.I., Goring, D.G., Biggs, B.J.F., 1997. On stream periphyton-turbulence interactions. N. Z. J. Mar. Freshwat. Res. 31, 435–448.

Nikora, V., Green, M.O., Thrush, S.F., Hume, T.M., Goring, D., 2002. Structure of the internal boundary layer over a patch of pinnid bivalves (*Atrina zelandica*) in an estuary. J. Mar. Res. 60, 121–150.

O'Riordan, C.A., Monismith, S.G., Koseff, J.R., 1993. A study of concentration boundary-layer formation over a bed of model bivalves. Limnol. Oceanogr. 38, 1712–1729.

O'Riordan, C.A., Monismith, S.G., Koseff, J.R., 1995. The effect of bivalve excurrent jet dynamics on mass transfer in a benthic boundary layer. Limnol. Oceanogr. 40, 330–344.

Prins, T.C., Smaal, A.C., Pouwer, A.J., Dankers, N., 1996. Filtration and resuspension of particulate matter and phytoplankton on an intertidal mussel bed in the Oosterschelde estuary (SW Netherlands). Mar. Ecol. Prog. Ser. 142, 121–134.

Riisgård, H.U., 1991. Filtration rate and growth in the blue mussel, *Mytilus edulis* Linneaus, 1758: dependence on algal concentration. J. Shellfish Res. 10, 29–35.

Riisgård, H.U., Larsen, P.S., 2001. Minireview: Ciliary filter feeding and bio-fluid mechanics- present understanding and unsolved problems. Limnol. Oceanogr. 46, 882–891.

Schlichting, H., 1979. Boundary Layer Theory, vol. 7. McGraw-Hill, New York.

Soulsby, R.L., Dyer, K.R., 1981. The form of the near-bed velocity profile in a tidally accelerating flow. J. Geophys. Res. 86, 8067–8074.

Springer, B., Friedrichs, M., Graf, G., Nittikowski, J., Queisser, W., 1999. A high precision current measurement system for laboratory flume systems: a case study around a circular cylinder. Mar. Ecol. Prog. Ser. 183, 305–310.

Stamhuis, E.J., Videler, J.J., 1995. Quantitative flow analysis around aquatic animals using laser sheet particle image velocimetry. J. Exp. Biol. 198, 283–294.

Tennekes, H., Lumley, J.L., 1999. A First Course in Turbulence, vol. 17. MIT Press, Massachusetts Institute of Technology, Cambridge, Massachusetts.

Widdows, J., Brinsley, M., 2002. Impact of biotic and abiotic processes on sediment dynamics and the consequences to the structure and functioning of the intertidal zone. J. Sea Res. 48, 143–156.

Widdows, J., Lucas, J.S., Brinsley, M.D., Salkeld, P.N., Staff, F.J., 2002. Investigation of the effects of current velocity on mussel feeding and mussel bed stability using an annular flume. Helgoland Mar. Res. 56, 3–12.

Wildish, D.J., Kristmanson, D., 1997. Benthic Suspension Feeders and Flow. Cambridge University Press, Cambridge.

Wildish, D.J., Miyares, M.P., 1990. Filtration rate of blue mussel as a function of flow velocity: preliminary experiments. J. Exp. Mar. Biol. Ecol. 142, 213–219.

Wright, L.D., Schaffner, L.C., Maa, J.P.Y., 1997a. Biological mediation of bottom boundary layer processes and sediment suspension in the lower Chesapeake Bay. Mar. Geol. 141, 27–50.

Wright, L.D., Friedrichs, C.T., Hepworth, D.A., 1997b. Effects of benthic biology on bottom boundary layer processes, Dry Tortugas Bank, Florida Keys. Geo-Mar. Lett. 17, 291–298.